ARL-TR-9594 ● Oct 2022

DEVCOM ARMY RESEARCH LABORATORY

Conversion of a User-Defined Bone Material Model from Abaqus to LS-DYNA

by Carolyn E Hampton, Stephen L Alexander, and Tusit Weerasooriya

Approved for public release: distribution unlimited.

NOTICES

Disclaimers

The research reported in this document was performed in connection with contract/instrument W15P7T-19-D-0126 with the Combat Capabilities Development Command (DEVCOM) Army Research Laboratory.

The findings in this report are not to be construed as an official Department of the Army position unless so designated by other authorized documents. The views and conclusions contained in this document are those of SURVICE Engineering Company and the DEVCOM Army Research Laboratory.

Citation of manufacturer's or trade names does not constitute an official endorsement or approval of the use thereof.

Destroy this report when it is no longer needed. Do not return it to the originator.

ARL-TR-9594 ● OCT 2022

Conversion of a User-Defined Bone Material Model from Abaqus to LS-DYNA

Carolyn E Hampton and Tusit Weerasooriya
DEVCOM Army Research Laboratory

Stephen L Alexander
SURVICE Engineering Company

Approved for public release: distribution unlimited.

REPORT DOCUMENTATION PAGE

Form Approved
OMB No. 0704-0188

Public reporting burden for this collection of information is estimated to average 1 hour per response, including the time for reviewing instructions, searching existing data sources, gathering and maintaining the data needed, and completing and reviewing the collection information. Send comments regarding this burden estimate or any other aspect of this collection of information, including suggestions for reducing the burden, to Department of Defense, Washington Headquarters Services, Directorate for Information Operations and Reports (0704-0188), 1215 Jefferson Davis Highway, Suite 1204, Arlington, VA 22202-4302. Respondents should be aware that notwithstanding any other provision of law, no person shall be subject to any penalty for failing to comply with a collection of information if it does not display a currently valid OMB control number.
PLEASE DO NOT RETURN YOUR FORM TO THE ABOVE ADDRESS.

1. REPORT DATE *(DD-MM-YYYY)*	2. REPORT TYPE	3. DATES COVERED (From - To)
September 2022	Technical Report	1 April 2021–31 August 2022

4. TITLE AND SUBTITLE
Conversion of a User-Defined Bone Material Model from Abaqus to LS-DYNA

5a. CONTRACT NUMBER

5b. GRANT NUMBER

5c. PROGRAM ELEMENT NUMBER

6. AUTHOR(S)
Carolyn E Hampton, Stephen L Alexander, and Tusit Weerasooriya

5d. PROJECT NUMBER

5e. TASK NUMBER

5f. WORK UNIT NUMBER

7. PERFORMING ORGANIZATION NAME(S) AND ADDRESS(ES)
DEVCOM Army Research Laboratory
ATTN: FCDD-RLW-TB
Aberdeen Proving Ground, MD 21005

8. PERFORMING ORGANIZATION REPORT NUMBER
ARL-TR-9594

9. SPONSORING/MONITORING AGENCY NAME(S) AND ADDRESS(ES)

10. SPONSOR/MONITOR'S ACRONYM(S)

11. SPONSOR/MONITOR'S REPORT NUMBER(S)

12. DISTRIBUTION/AVAILABILITY STATEMENT
Approved for public release: distribution unlimited.

13. SUPPLEMENTARY NOTES
ORCID IDs: Carolyn E Hampton, 0000-0002-7246-2488; Tusit Weerasooriya, 0000-0003-3299-2166

14. ABSTRACT

DEVCOM Army Research Laboratory researchers had previously developed Abaqus user-defined material models for human bone that could capture the failure behavior observed from experiments. This study aims to translate these materials for use with the LS-DYNA finite element software in support of broader use and validation efforts. After successful translation, four test cases were simulated in LS-DYNA to demonstrate the equivalence between the LS-DYNA and Abaqus material model. These four test cases were a combination of one of two specimens (a cuboid bone block and a hemispherical section of parietal skull) and material model implementations (VUMAT A or B). The simulations with VUMAT A agreed well with the previously published Abaqus results in peak force, time of failure, and extent of failure cascades. The simulations with VUMAT B were very similar as well, with dependencies on the contact implementation and time-step control identified as possible causes for the variations in force-displacement response. The linear crack initiation and propagation behavior was successfully reproduced in both VUMATs. Several appendixes provide further instruction in compiling and using the new LS-DYNA materials in other applications.

15. SUBJECT TERMS
Mechanical Sciences, Sciences of Extreme Materials, biomaterials, biomechanics, bone, material property, skull fracture, LS-DYNA, user-defined material model, finite element, uniaxial compression

16. SECURITY CLASSIFICATION OF:			17. LIMITATION OF ABSTRACT	18. NUMBER OF PAGES	19a. NAME OF RESPONSIBLE PERSON
a. REPORT	b. ABSTRACT	c. THIS PAGE			Carolyn E Hampton
Unclassified	Unclassified	Unclassified	UU	52	19b. TELEPHONE NUMBER (Include area code) (540) 449-8801

Standard Form 298 (Rev. 8/98)
Prescribed by ANSI Std. Z39.18

Contents

List of Figures

List of Tables

Acknowledgments

The authors would like to acknowledge the assistance of fellow ARL researchers Alan Goertz and Brian Fagan for assistance with writing Fortran 77 code and subfunctions and Alan Goertz for guidance on distributing and compiling the LS-DYNA executables on the Centennial cluster, which greatly expedited the material conversion process.

1. Introduction

Head injuries account for a significant portion of Army casualties. A common injury mechanism is blunt trauma caused by the interaction between the deforming helmet and the head and skull. The US Army Combat Capabilities Development Command (DEVCOM) Army Research Laboratory (ARL) has been using computational finite element methods to study the injury mechanisms leading to these injuries. A major challenge in this approach has been the development of a mathematical material model that can capture the complex behaviors of biological tissues, especially those of skin and bone.

Such models are typically developed from experimental characterization of the bone under consideration. Some of the oldest models were linear elastic relationships based on mechanical testing of whole bones (McElhaney 1966). Recent ARL efforts have focused on characterizing the response of human skull under compressive loading (Gunnarsson et al. 2021) but at a resolution where the changes in density throughout the different layers become significant. The human skull is generally considered to contain three layers through the thickness. From the outside to inside, these layers are the outer table, diploe, and inner table. While the two tables are dense bone, the interior diploe layer is extremely porous, which is reflected by a low bone volume density. The change in density is not discrete and was found to follow a U-shaped curve when presented as density versus depth (Alexander et al. 2019).

The experimental work to characterize the human skull culminated in a custom user-defined finite element material model implemented in Abaqus to simulate uniaxial compression of through-thickness sections of skull (Alexander and Weerasooriya 2021). This material was built upon a conventional linear elastic theory. However, it included a new mechanism that automated the adjustment of the material properties in accordance with the bone volume fraction (BVF) associated with each element. This approach enabled modeling of both the true bone volume gradient and large voids that exist within real skull bone.

Shortly after, the new skull material model was used in an indentation simulation of a hemispherical skullcap section, intended to be a more realistic depiction of potentially injurious impacts (Weerasooriya and Alexander 2021). The indentation loading was more complex than the previous uniaxial compression testing, and a new version of the user material was developed to improve the response in combined tension, compression, and shear loading (Alexander et al. 2021).

The skull user material model was implemented in the Abaqus finite element software, whereas other groups (both ARL and non-ARL) use the LS-DYNA finite element software. This study focused on reproducing the Abaqus user material

model for human skull as an LS-DYNA user material model. The previously published simulations were recreated as LS-DYNA simulations so that the equivalence of the two material models could be demonstrated by comparing against the original Abaqus results.

2. Methods

The LS-DYNA user material (Livermore Software Technology [LST] 2020) was written in Fortran 77 to ensure compatibility with the LS-DYNA source code, which was based on the original DYNA3D code written in the 1970s (Hallquist and Whirley 1989). The input format and instructions to use the already compiled material models are described in Appendixes A and B. A compiling guide for users wishing to build their own local executable, and potentially make their own modifications, is in Appendix C.

Development of the finite element models for this study was completed with the HyperMesh preprocessing software (Altair Engineering, Inc). Simulations were run with a user-compiled version of LS-DYNA R12.0.0 (LST 2020) that included the user-defined material models developed for this study. The unit system for all simulations was mm-kg-ms, with implied units of kN-GPa-J. Postprocessing of results was performed with LS-PrePost software (Ansys International, Inc) and MATLAB software (MathWorks, Inc). Some contours were collected in HyperView (Altair Engineering, Inc), which allowed for custom color bars to match the contours from the literature.

Unless otherwise noted, the simulation settings were as follows. Each uniaxial compression of bone block simulation was run on Centennial computing cluster with four processors, which took about 5 min to finish per simulation. Each indentation of skullcap simulation was run on the Centennial cluster with 32 processors, which required 20–60 min per simulation. Commonly employed controls for highly distorted elements such as time step–based erosion were not used. The full list of simulations can be found in Appendix D.

Each simulation used one of four test cases defined by the permutation of specimen (bone block or skullcap) and user-defined material (VUMAT A or B) options. Most of these cases have a corresponding publication (Table 1) except for one case where an additional ABAQUS simulation was run to provide validation data.

Table 1 All the Abaqus simulations reproduced in this study as LS-DYNA simulations

Loading mechanism	Specimen	User material	Literature reference
Uniaxial compression	Bone block	VUMAT A	Alexander and Weerasooriya 2021
Uniaxial compression	Bone block	VUMAT B	None
Uniaxial indentation	Skullcap	VUMAT A	Weerasooriya and Alexander 2021
Uniaxial indentation	Skullcap	VUMAT B	Alexander et al. 2021

2.1 Uniaxial Compression of Bone Block with VUMAT A

This model was based on the works of Alexander and Weerasooriya (2021) in which a cuboid of skull bone was subjected to near-quasistatic uniaxial compression. The exact mesh used for the Abaqus model (Fig. 1) was provided as a starting point for the LS-DYNA finite element model. The 16,683 tetrahedral elements represented a full-thickness block of skull bone measuring 5.774 × 6.878 × 9.255 mm. The initial contact area on the top surface was 39.71 mm^2. The tetrahedral elements were segmented into one of 101 materials, each with a different BVF ranging from 0 to 1 in increments of 0.01. The material with an impermissible BVF of 0 was reassigned a value of 0.001. These BVF values, along with the reference material properties of 100% dense bone, could be used to calculate all the adjusted material properties needed to capture the mechanical strength of porous bone. The element formulation for all tetrahedral elements was changed from the default to the one-point tetrahedron (ElForm 10). Note the coordinate system used in this study differed from the referenced source study, such that the uniaxial compression here was applied in the Z-axis as opposed to the Y-axis.

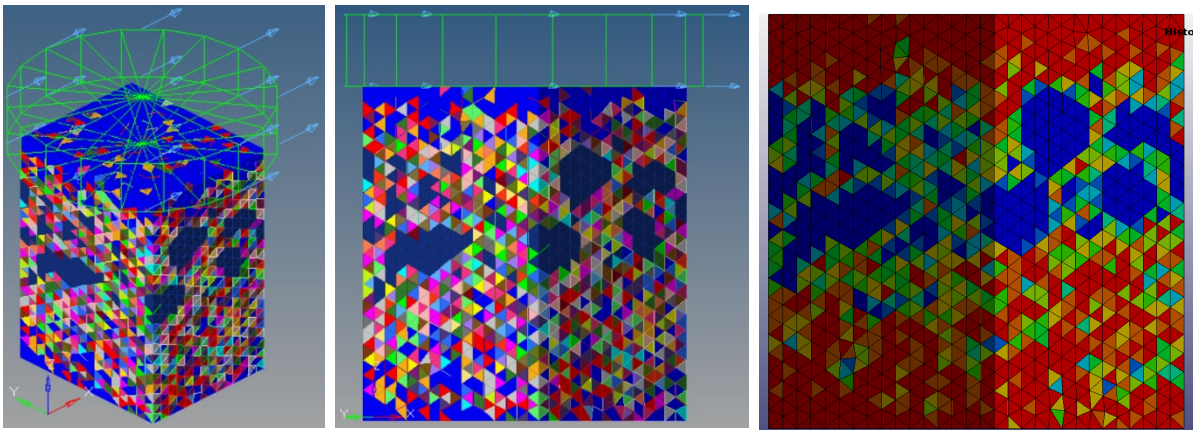

Fig. 1 Different HyperMesh views of the bone block model (left and center) with pseudocolors differentiating the 101 materials. The colored contour (right) shows the BVF of each element in the middle image.

The boundary conditions as defined in Abaqus were not imported and needed to be recreated. The circular platen applying the uniaxial compression was recreated as a moving rigid geometric body through the RIGIDWALL_GEOMETRIC_ CYLINDER_MOTION_DISPLAY card. This rigid wall moved with a linear prescribed displacement over time, uniaxially compressing the top face nodes of the bone block. The applied displacement increased linearly, reaching 0.055532 mm (an engineering strain of 0.6%) by the simulation end. Generic linear elastic material properties for steel ($\rho = 7.8*10^{-6}$ kg/mm^3, E = 200 GPa, $\nu = 0.28$) were added for computing contact forces and time steps. The bottom platen, which did not move at all, was replaced with a RIGIDWALL_PLANAR card that supported the nodes in the bottom face. Both rigid walls were assigned friction coefficients of 0.1.

The LS-DYNA model was set to run 5 ms of simulated time. Contact force, global energies, and select nodal kinematics were recorded at 1 MHz (0.001 ms/sample). Visual states were written every 0.005 ms (200 kHz). The global bulk viscosity coefficient Q1 was changed from the default 1.0 to 1.2 to match the Abaqus default value.

Material properties that were shared between the 101 different user-defined bone material models are shown in Table 2. LS-DYNA required that certain properties (density, bulk modulus, and shear modulus) be provided during initialization to calculate the initial element time steps, resulting in this material model having more inputs than the corresponding Abaqus model. Refer to Appendix A for a guide on using LS-DYNA VUMAT A, which includes the layout and meaning of the material parameters. The reference shear failure limit (REFSFS) was not part of the Abaqus VUMAT A when Alexander and Weerasooriya (2021) was published, but was included in later versions of VUMAT A. Thus, the parameter was present here but was set to an unreachable value of 99999 to disable this failure mechanic.

Table 2 LS-DYNA user material cards to simulate bone block without failure options using VUMAT A

MID	RO	MT	LMC	NHV	IORTHO	IBULK	IG
various	various	41	14	3	0	7	8
IVECT	IFAIL	ITHERM	IHYPER	IEOS	LMCA		
1							
BVF	EXPN	EXPK				K	G
various	1.585	2.0				various	various
REFRO	REFMOD	REFNU	REFSFC	REFSFT	REFSFS		
1.8E-6	8.528	0.3	0.175	0.175	99999		

An additional simulation was run with the failure limits of the reference bone in compression (REFSC) and tension (REFST) also set to an arbitrarily high value (99999) so that the failure mechanics could not activate during the simulation. The max displacement was also lowered to 0.03702 mm (engineering strain of 0.4%). This simulation corresponded to the preliminary Abaqus simulation of linear response in Alexander and Weerasooriya (2021).

2.2 Uniaxial Compression of Bone Block with VUMAT B

The 0.6% uniaxial compression simulation of the bone block was run again but with a different user-defined material model. The new material model, called VUMAT B, was first described in Alexander et al. (2021) and used to simulate the response of a hemispherical cutout of human skull. This material model was extracted and retro-actively applied to the bone block under uniaxial compression. Unpublished data from the corresponding Abaqus simulation of the bone block with VUMAT B was provided for this study. The new format for the VUMAT B user material model is shown in Table 3. Refer to Appendix B for a guide on using this LS-DYNA version of VUMAT B, which includes the layout and meaning of the parameters for this user material model.

Aside from the transition from VUMAT A to VUMAT B, the following changes were made to the bone block model:

- The modulus exponent (EXPN) has changed from 1.585 to 1.603
- The lowest BVF material has changed from a BVF of 0.001 to 0.005

Table 3 LS-DYNA user material cards to simulation bone block with VUMAT B

MID	RO	MT	LMC	NHV	IORTHO	IBULK	IG
various	various	44	15	3	0	7	8
IVECT	IFAIL	ITHERM	IHYPER	IEOS	LMCA		
1							
BVF	EXPN	EXPK	SRATE	A	HFLR	K	G
various	1.603	2.0	10000	0.998	1E-4	various	various
REFRO	REFMOD	REFNU	REFSFC	REFSFT	REFSFS	REFSFR	
1.8E-6	8.528	0.3	0.175	0.175	0.15	0.48	

2.3 Skullcap Indentation with VUMAT A

The bone block was replaced by a more biofidelic section of human skull (Weerasooriya and Alexander 2021) in which the VUMAT A user material model was used to model the skullcap material. The physical experiments upon which this model was based are described by Gunnarsson et al. (2021). The exact same meshes for the right parietal skull cap specimen LR08 and aluminum support plate were

provided and are shown in Fig. 2. The skullcap mesh contained 230,924 tetrahedral elements and measured 88.82 mm long, 71.65 mm wide, and 9.24 mm tall. The skullcap was created with 100 different materials, ranging from a BVF of 0.005 to 0.995 in increments of 0.005.

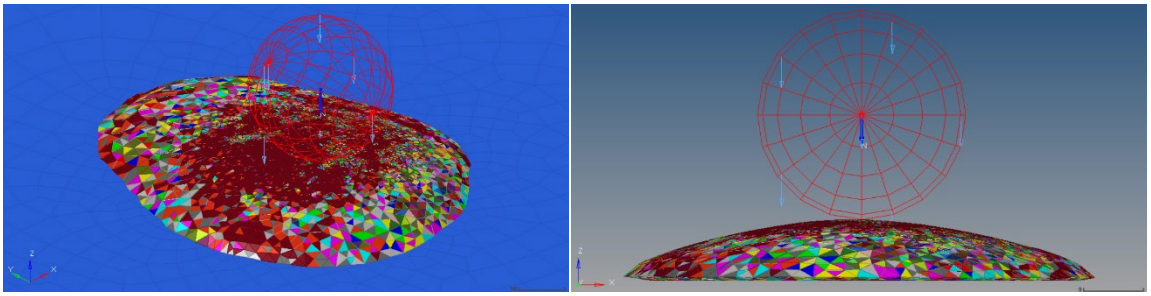

Fig. 2 Skullcap finite element model. Pseudocolors assigned for skullcap materials with different initial BVFs.

The skullcap was supported by a deformable aluminum plate (200 × 200 × 9.6 mm). The plate was assigned linear elastic material properties for aluminum (ρ = 2,720 kg/m^3, E = 69 GPa, ν = 0.35). Two contacts between the skullcap-plate and skullcap-indenter were both assigned friction coefficients of 0.1.

LS-DYNA did not have a geometric hemisphere option, so a 31.75-mm-diameter geometric sphere was added to represent the indenter (RIGIDWALL_GEOMETRIC_SPHERE_MOTION card). The previously described linear elastic material properties for steel were assigned to the indenter, which moved with a sine-like prescribed displacement applied over 10 ms (Fig. 3).

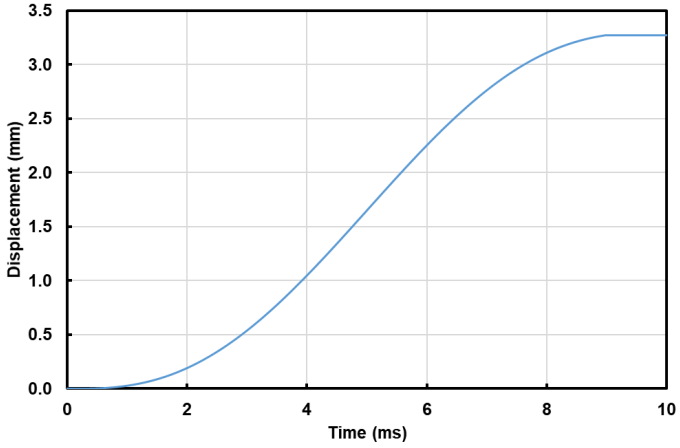

Fig. 3 Prescribed motion of the rigid indenter over time

The new user material card for this simulation is shown in Table 4. The following parameters have changed from the previous uniaxial compression of the bone block with VUMAT B simulation:

- The reference elastic modulus (REFMOD) has dropped to 3.0 GPa
- The reference tensile failure limit has increased to 269.4 MPa

Table 4 LS-DYNA user material cards for skullcap indentation with VUMAT A

MID	RO	MT	LMC	NHV	IORTHO	IBULK	IG
various	various	41	14	3	0	7	8
IVECT	IFAIL	ITHERM	IHYPER	IEOS	LMCA		
1							
BVF	EXPN	EXPK				K	G
various	1.603	2.0				various	various
REFRO	REFMOD	REFNU	REFSFC	REFSFT	REFSFS		
1.8E-6	3.0	0.3	0.175	0.2694	0.15		

2.4 Skullcap Indentation with VUMAT B

The final Abaqus model under consideration was published in Alexander et al. (2021). In this simulation, the skullcap model was subjected to identical loading conditions, but the new user-defined VUMAT B material model implemented a cumulative damage routine to smooth out element failure cascades and generate more realistic fracture patterns.

The corresponding LS-DYNA skullcap indentation simulation was updated to use the material cards shown in Table 5. There were no changes to the reference material properties of 100% dense bone.

Table 5 LS-DYNA user material cards for skullcap indentation with VUMAT B

MID	RO	MT	LMC	NHV	IORTHO	IBULK	IG
various	various	44	15	3	0	7	8
IVECT	IFAIL	ITHERM	IHYPER	IEOS	LMCA		
1							
BVF	EXPN	EXPK	SRATE	A	HFLR	K	G
various	1.603	2.0	10000	0.998	1E-4	various	various
REFRO	REFMOD	REFNU	REFSFC	REFSFT	REFSFS	REFSFR	
1.8E-6	3.0	0.3	0.175	0.2694	0.15	0.48	

2.5 Data Processing

All simulations reported displacement by tracking the motion of the moving rigid wall, as this corresponded to the motion of the platen in the experiments. In most cases, there were small gaps between the platen and specimen at the beginning of each simulation. This gap was removed when processing the data in MATLAB. The displacements, strains, and times in the following sections reflect the adjustments to remove initial gap.

3. Results

3.1 Uniaxial Compression of Bone Block with VUMAT A

Examples of the typical global energy balances (Fig. 4) showed growth in the simulation energy, which is typical of simulations driven by prescribed motions. Internal energy made up most of the total energy in the form of specimen deformation, with the other energy modes being near zero. The smoothness of the curves and the minimal amounts of contact and hourglass energies indicated that this simulation was stable. The minimal kinetic energy meant that this simulation was a reasonable approximation of the quasistatic experiments.

The energy curves for the skullcap simulation were less smooth, which was a common indicator of unloading and reloading as individual elements undergo failure. The skullcap simulation also had nonzero, but still relatively low, energies dissipated as friction in the sliding contacts.

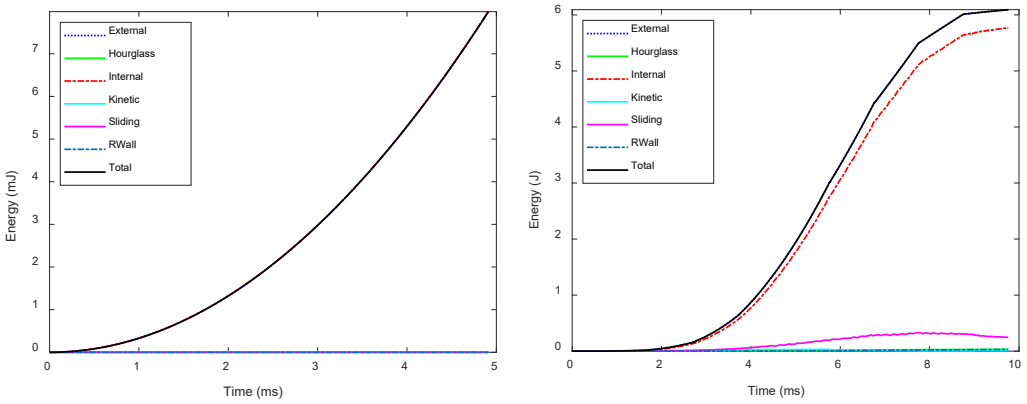

Fig. 4 Examples of global energy balances for a uniaxial compression of bone block with VUMAT A simulation with failure disabled (left) and a skullcap indentation with VUMAT B simulation (right)

The simulation contact force between the moving platen and bone block was converted to engineering stress. Similarly, the applied displacement was converted to an engineering strain. The resulting cross-plot of stress–strain (Fig. 5) showed excellent agreement between the LS-DYNA and Abaqus user material models, where both report that the effective modulus of the whole bone block was 2.82 GPa. This is 33% of the reference modulus of purely dense bone but can be different whenever the finite element mesh changes.

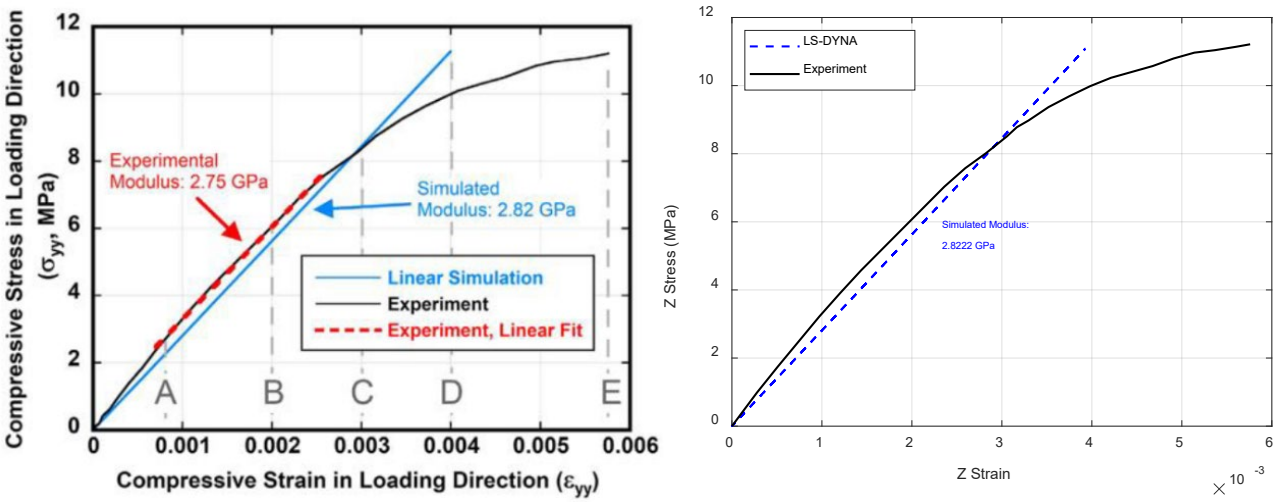

Fig. 5 No-failure results from the Abaqus simulation (left) and the corresponding LS-DYNA model (right)

Once the compressive and tensile failure limits were restored, the LS-DYNA simulation was successful in reproducing the behavior of the equivalent Abaqus mode as shown in Fig. 6. The peak stress within the block was 11.44 MPa, which occurred at 0.46% strain or 3.92 ms in the LS-DYNA simulation. After this point, both the LS-DYNA and Abaqus simulations went through a series of element failure cascades in which the block cycled between slowly reloading and load-shifting failure cascades until the end of the simulation. None of the peak stresses in the subsequent cycles reached the first peak stress.

The figure also shows the cumulative number of failed elements over time. Most of the elements failed in compression, and sudden spikes in the number of elements that failed corresponded to a stress drop in the block. A total of 2,818 elements failed in the LS-DYNA simulation, of which 2,578 were from compression and only 240 from tension. The Abaqus failed element counts were not available, but visually there was excellent agreement in both cumulative number of failed elements and timing of the failure cascades.

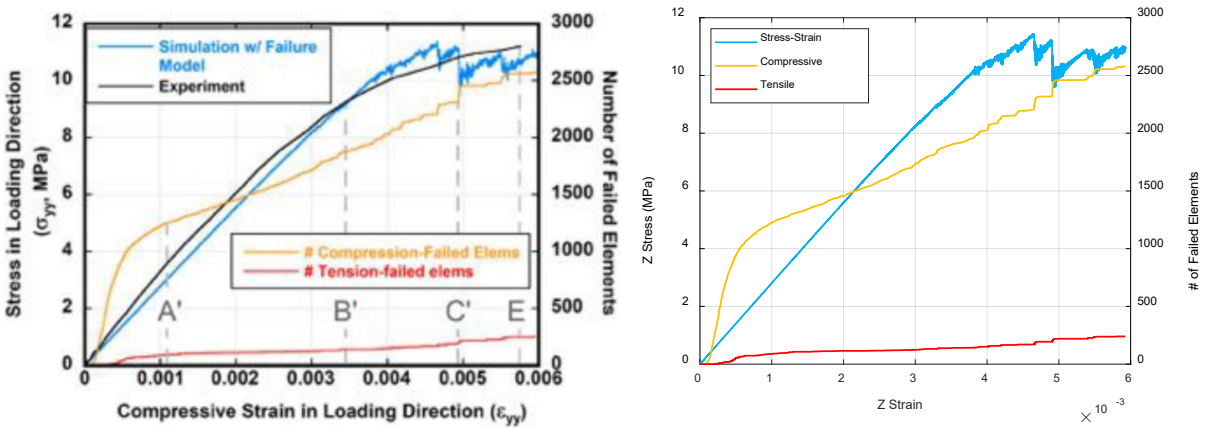

Fig. 6 Stress–strain response and failed elements in Abaqus (left) and LS-DYNA (right) for uniaxial block with VUMAT A

The global Z-strain contours for the bone block are shown in Fig. 7. The majority of elements carried compressive strains, as failed elements continue to sustain some bulk loading while the remaining load was shunted toward the remaining healthy elements. Strains were higher in the middle diploe layer as this layer had lower BVFs. Most of the elements in tension were also found in this layer. However, the block as a whole sustained loading and never suffered a gross failure prior to reaching the maximum prescribed strain. Some elements that failed in tension were highly distorted near the end of the LS-DYNA simulation, but these elements did not affect the overall response and can be masked if needed.

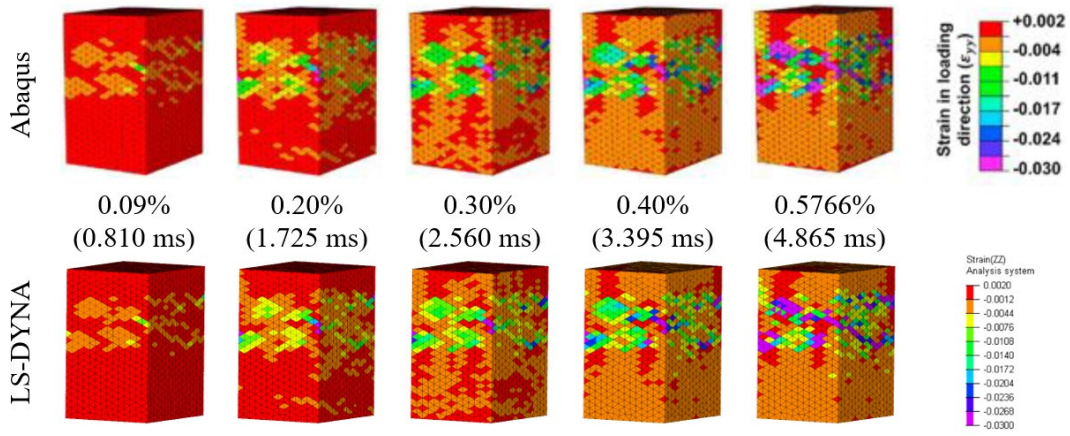

Fig. 7 Z-strain contours in Abaqus (top line) and LS-DYNA (bottom line) for uniaxial block with VUMAT A. The corresponding Z-strain and time for each column are in the middle lines. Contours were projected onto the undeformed mesh.

3.2 Uniaxial Compression of Bone Block with VUMAT B

The stress–strain response of the block with VUMAT B (Fig. 8) was very similar to the previous simulation with VUMAT A (Fig. 6). The peak stress was slightly lower at 11.40 MPa and occurred later in the simulation at 4.11 ms / 0.49% strain. After this peak was reached, a similar pattern of failure cascades and slow reloading was observed.

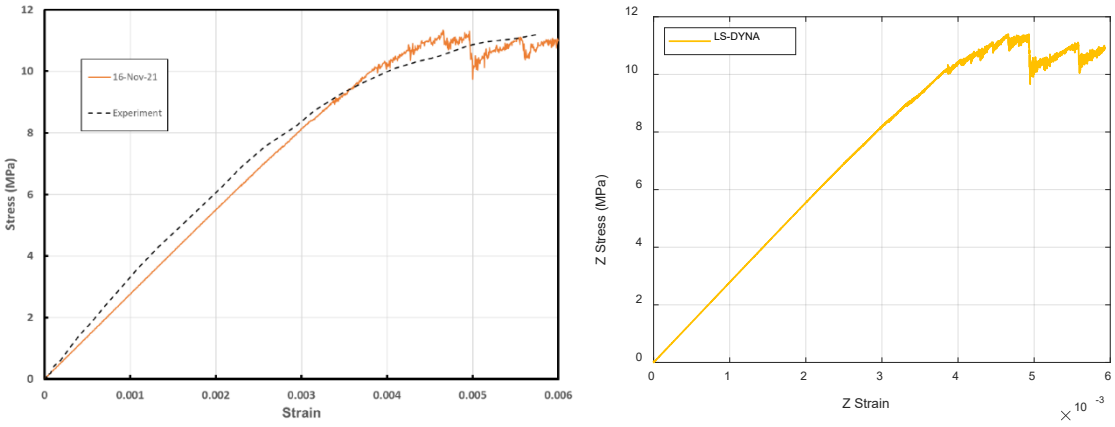

Fig. 8 Stress–strain profiles from Abaqus (left) or LS-DYNA (right) for uniaxial block with VUMAT B

Table 6 shows the first six elements to fail in each simulation, and the time at which they failed. In LS-DYNA, these elements were exclusively low BVF elements in the diploe layer. The timing of the first element to fail is different. The reason was unclear but may be due to differences in a larger initial gap between the top platen and the bone block in the LS-DYNA model.

Table 6 The first six elements to fail for uniaxial block with VUMAT B

Abaqus			LS-DYNA		
Elem. no.	**Time (ms)**	**Mechanism**	**Elem. no.**	**Time (ms)**	**Mechanism**
NA	0.15794	Compression	8560	0.15581	Compression
NA	0.16210	Compression	3233	0.15956	Compression
NA	0.16236	Compression	8997	0.16002	Compression
NA	0.16277	Compression	10961	0.16146	Compression
NA	0.16438	Compression	5588	0.16227	Compression
NA	0.16854	Compression	11641	0.16822	Compression

Ultimately, 2,797 elements failed in the Abaqus simulation. Of these, 2.501 failed in compression, 222 in tension, and 74 in shear. In LS-DYNA, a total of 2,812 elements failed. Of these, 2,511 failed in compression, 224 in tension, and 77 in shear. Again, the overall response was nearly identical, while there were some subtle

differences in the timing for failed elements. It is unclear if this timing difference was due to different initial gaps between the block and platen.

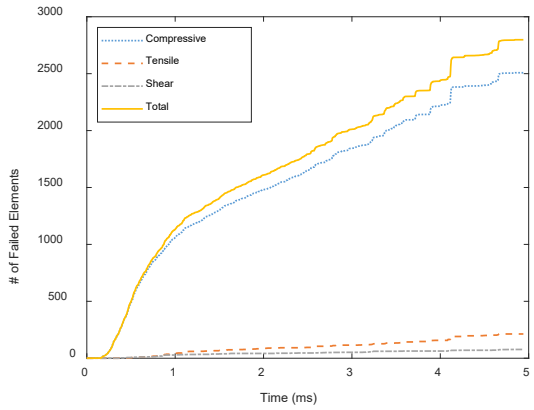

Fig. 9 Tally of failed elements in LS-DYNA for uniaxial block with VUMAT B

The LS-DYNA elements that failed are shown in Fig. 10. Nearly all of the elements were concentrated in the middle of the bone block where the BVF was low. The element health (damage in the Abaqus version) is also shown, and the vast majority of elements had the same health. This was expected since the health is only updated for elements in tension, which should be uncommon in a uniaxial compression test. However, it was not zero due to the complex microstructure, and several elements with reduced health can be seen on the faces of the bone block.

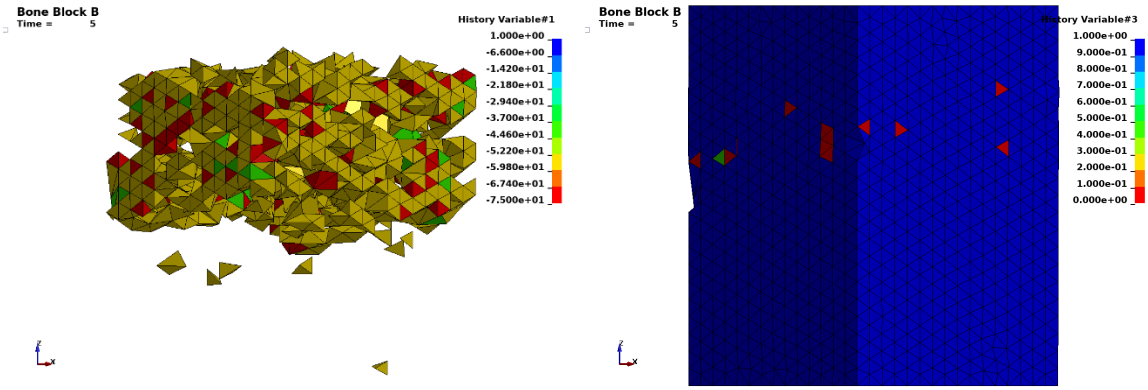

Fig. 10 All LS-DYNA failed elements and their states at the end of the simulation (left). The health of each element at the end of the simulation (right).

3.3 Skullcap Indentation with VUMAT A

The response of the hemispherical skullcap simulation with VUMAT A was similar to that of the bone block, where there was a roughly linear response until the element failure cascades begin. Since the hemispherical shape precludes an easy calculation of global strain, the force-displacement results were reported instead of the previous

stress–strain (Fig. 11). The LS-DYNA simulation reached a peak force of 2.93 kN at 2.90 mm (7.18 ms), which occurred after the first failure cascade.

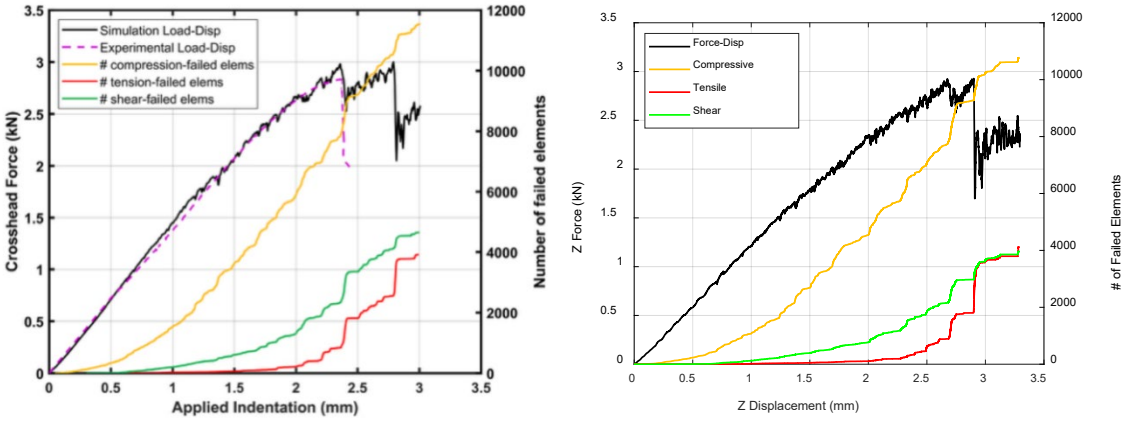

Fig. 11 Skullcap force-displacement in Abaqus (left) and LS-DYNA (right)

The arched shape for the skullcap allowed for more failure modes to appear, and the number of elements that failed in tension and shear were much higher than for the uniaxially loaded bone block (Fig. 11 vs. Fig. 6). However, compression remained the predominate failure mode. At the simulation end, a total of 18,851 elements had failed (10,769 in compression, 4,118 in tension, 3,964 in shear).

The fractures induced by the indentation are shown in in Fig. 12. At first, elements failed in compression directly under the impactor, followed by the lower BVF elements in the middle diploe layer. Soon after, the flexion induced by impactor resulted in tension failures in elements on the underside of the skullcap. These quickly propagated as cracks that occasionally branched when the crack tip encountered pockets of low BVF elements. This behavior was promising, as it matched the ABAQUS simulation results with experimental photo inset.

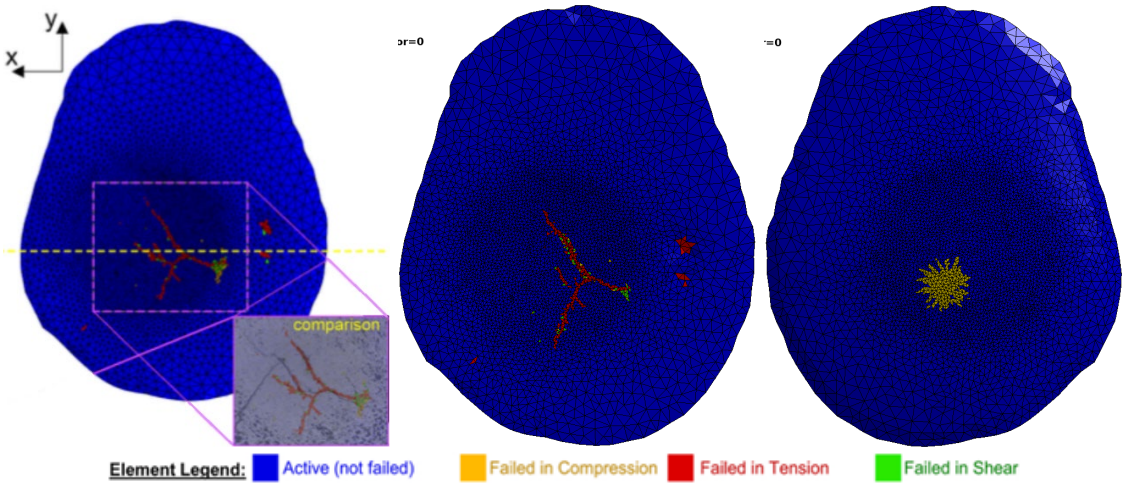

Fig. 12 Fracture patterns on underside of skullcap in Abaqus (left) and LS-DYNA (center) at 3-mm indentation, projected onto the undeformed mesh. The corresponding fracture pattern on the top surface in LS-DYNA also shown (right).

The overhead/underside views did not provide insight into the behavior of the middle layer, which was examined in Fig 13. The cross-sectional view revealed clustering of failed elements in the low BVF middle layer. Both the crush damage and tension cracks extend deep enough to combine with the middle layer, contributing to the large drops in the force-displacement curve. This mechanic might also lead to the production of comminuted fragments under larger loads.

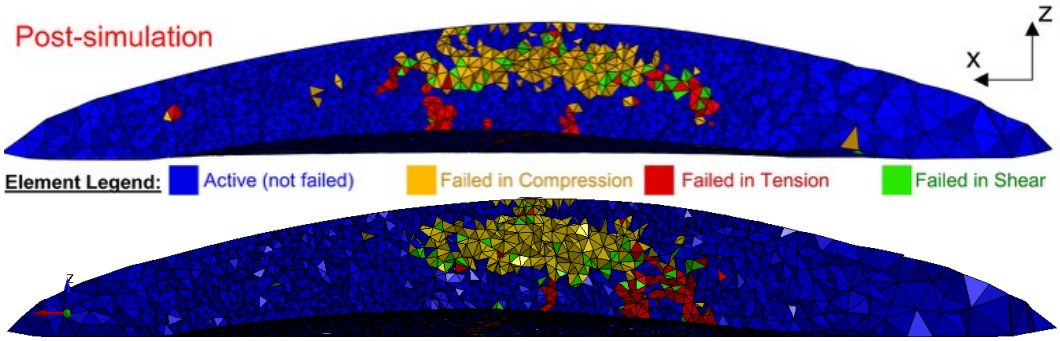

Fig. 13 Fracture patterns through the skullcap in the ZX plane at simulation end for Abaqus (top) and LS-DYNA (bottom). Contours projected onto the undeformed mesh.

3.4 Skullcap Indentation with VUMAT B

The force-displacement curves for the skullcap with VUMAT B simulations are shown in Fig. 14. The change from binary failure to gradual failure resulted in much smoother curves. The delay in failure allowed the simulations to reach a higher peak force, 3.27 kN in LS-DYNA, before beginning to decline. While this behavior was consistent with the smoother curve seen in the Abaqus simulations, it appeared to differ from the experimental behavior documented by Alexander et al. (2021).

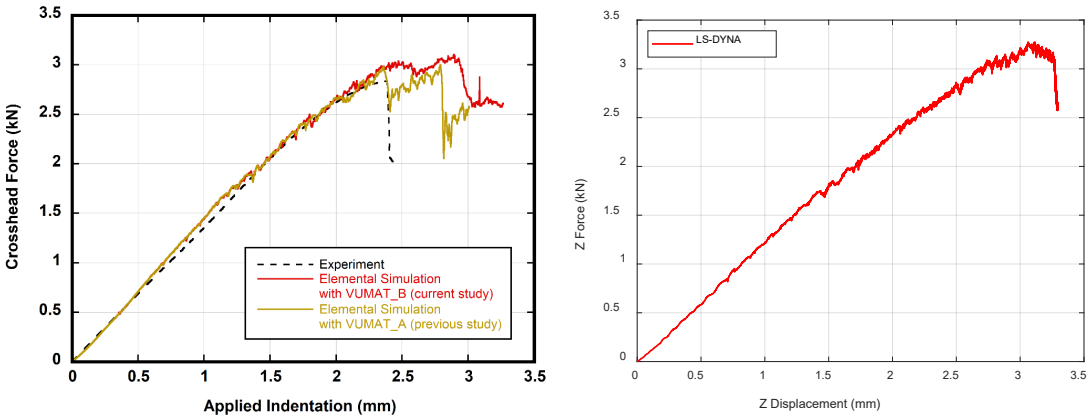

Fig. 14 Force-displacement from Abaqus (left, red line) and LS-DYNA (right) for skullcap with VUMAT B

A total of 19,485 elements failed during this LS-DYNA simulation (11,380 in compression, 3,316 in tension, and 4,762 in shear). The cumulative failed element tallies are shown in Fig. 15. The tally was slightly higher than recorded with VUMAT A (Fig. 11). However, this curve showed less of a trend toward leveling off.

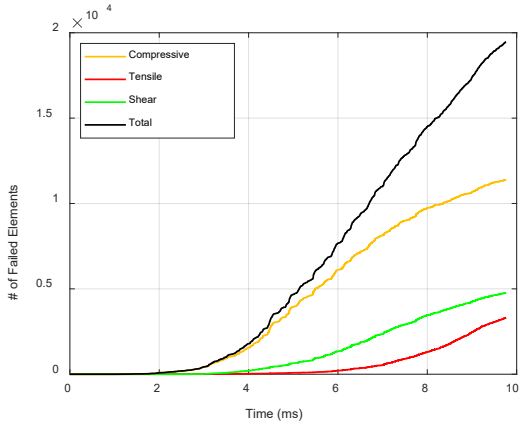

Fig. 15 Cumulative element failure over time in LS-DYNA for skullcap with VUMAT B

The fracture patterns between the LS-DYNA and Abaqus results were very similar, despite the large difference in the force-displacement results. The patterns are shown for 1, 2, and 3 mm of indentation in Fig. 16. Both LS-DYNA and Abaqus developed a vaguely “H” shaped crack on the underside of the skullcap (inner table). Elements associated with the cracks had failed primarily in tension, with the crack length increasing with more applied displacement. In contrast, the failed elements on the top surface (outer table) showed a spherical dent consisting of elements that failed in compression. The shape of the damaged area on the outer table likely reflected the spherical shape of the indenter.

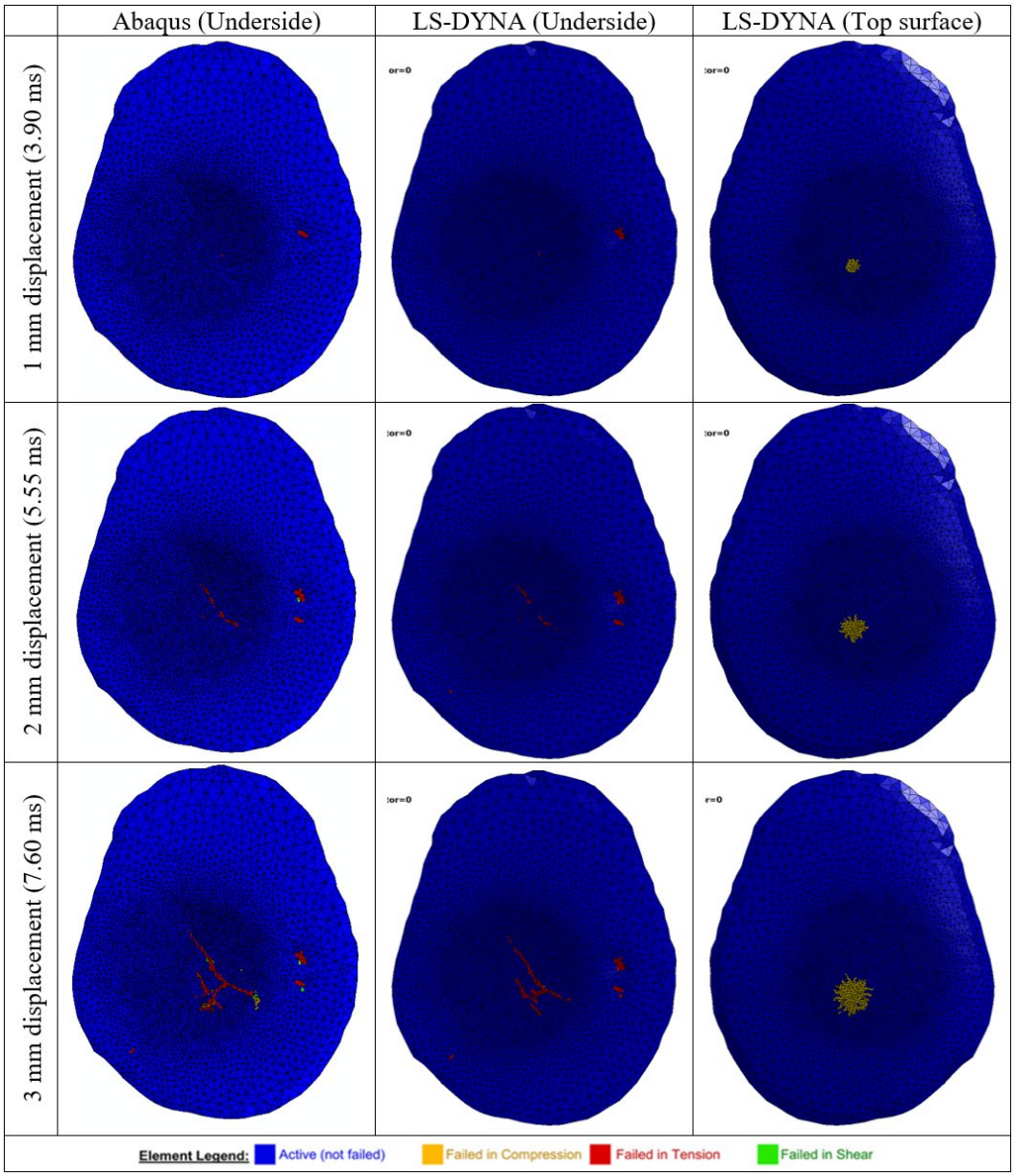

Fig. 16 Skullcap simulations showing element status at various levels of indentation projected onto the undeformed skullcap mesh. Colors indicate elements are healthy (blue) or have failed via compression (orange), tension (red), or shear (green).

The cross-sectional view (Fig. 17) shows that the element failures were concentrated in the central (diploe) layer, where the element densities were lower. The failed elements in this layer predominantly failed in compression with a smaller number of scattered elements failed in shear.

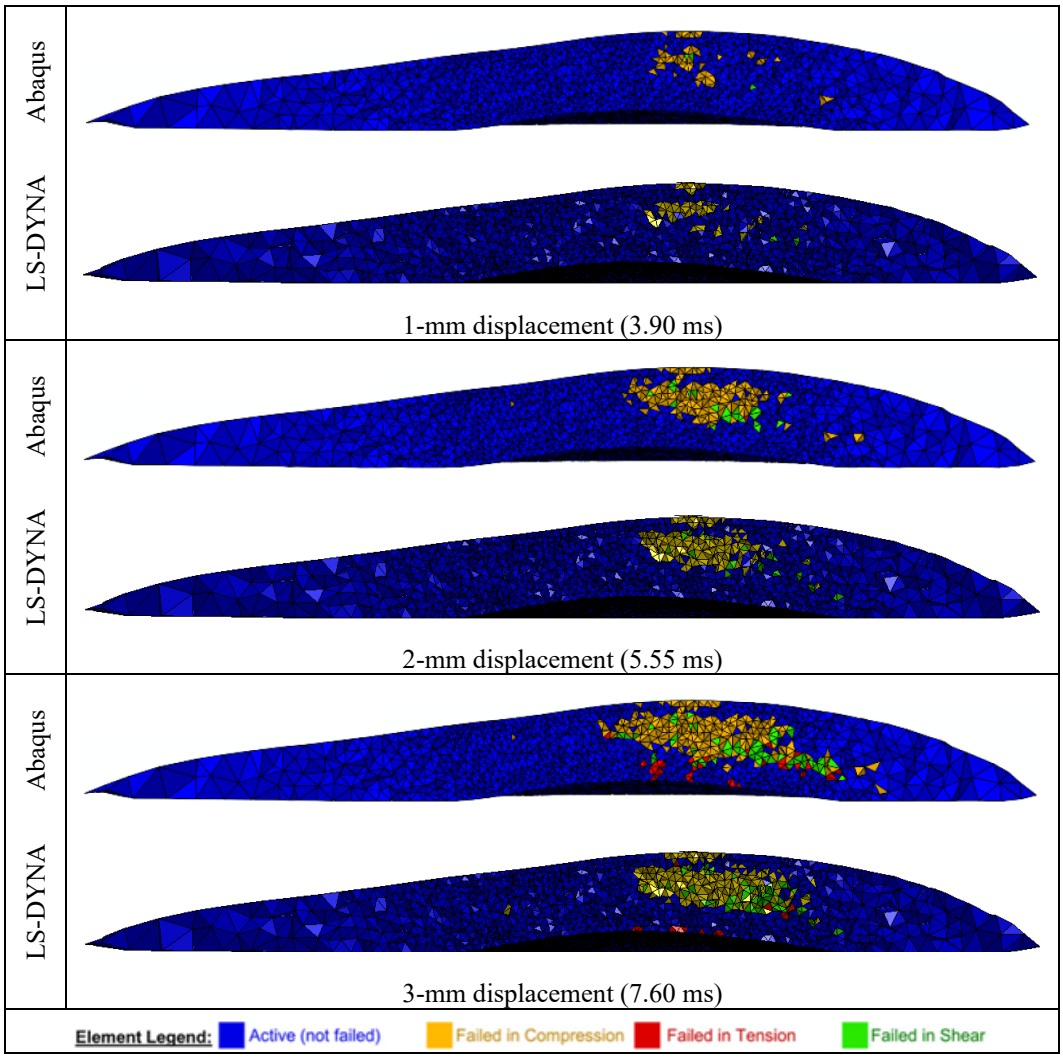

Fig. 17 Skullcap YZ plane cross-section element status at various times, projected onto the undeformed mesh. Colors indicate elements are healthy (blue) or have failed via compression (orange), tension (red), or shear (green).

4. Discussion

4.1 Erosion Implementation

In both VUMAT A and B, failed elements in compression lose the ability to support shear stress, and failed elements in tension cannot support any stress at all. This manifested as elements that quickly become highly distorted. Aside from being visible nonphysical behavior, this was problematic because such elements tend to drive the simulation time step down to zero or cause termination due to negative volume errors. Such elements were eventually controlled by implementation of a strain-rate-based erosion in the Abaqus VUMAT B. However, in LS-DYNA there

was a built-in time step–based erosion option that could be easily enabled by setting the ERODE and DTMIN fields. Three additional LS-DYNA skullcap with VUMAT B simulations were run to check the sensitivity of the results to element erosion. These simulations were (1) both time-step and strain rate erosion enabled, (2) time step–based erosion only, and (3) no erosion allowed. In simulations with time-step erosion, the cutoff was 10% of the original time step.

Figure 18 shows the force-displacement curves, which were largely unaffected by the particular erosion implementation used. The strain rate–based erosion was slightly quicker to erode some elements and resulted in the force drop occurring a tiny bit earlier. Combining the two erosion methods resulted in roughly the same results as either single method alone. On the other hand, running the simulation without any erosion was not successful. This simulation was only able to reach 6.5 out of 10 ms (2.49-mm displacement) before the time step fell to near zero. This was too soon to obtain useful information on the peak load and failure behavior, so running without any erosion control for bad elements would not be viable for these test cases. Given the minor differences seen in Fig. 18, there were also no differences in the visual fracture patterns, which were consistent with those from Fig. 16.

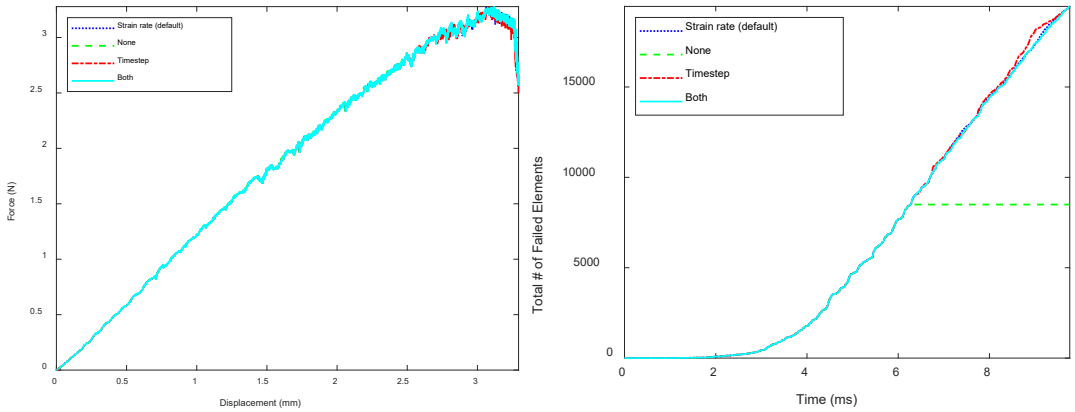

Fig. 18 LS-DYNA skullcap simulations with VUMAT B results for force-displacement (left) and total number of failed elements (right) with various methods of eroding distorted elements

Table 7 provided more details on the elements undergoing failure and erosion. The same seven elements eroded in the three erosion-enabled simulations. However, the strain rate check was the more aggressive of the two erosion criteria and was usually the first to erode elements when both criteria were enabled. Note that the strain rate check was only implemented for VUMAT B, so any simulations running with VUMAT A will benefit from using the time step–based erosion method. For example, running the skullcap with VUMAT A simulation without any erosion control resulted in the simulation time step falling from $4*10^{-5}$ ms to $4*10^{-20}$ ms

near 6.1 ms. While this did not result in an error termination, it had a similar effect as progress in the simulation was effectively halted.

Table 7 LS-DYNA changes in failed and eroded elements with different erosion options

Parameter	Default (strain rate only)	Both time step and strain rate	Time step only	No erosion
Comp failed	11,380	11,326	11,285	6,637
Tens failed	3,316	3,352	3,380	276
Shear failed	4,762	4,766	4,706	1,583
Total failed	19,458	19,444	19,371	8,496
Eroded (time step)	0	1	7	0
Eroded (strain rate)	7	6	0	0
Sim progress	100%	100%	100%	61%

Since the various erosion methods were successful in keeping the simulations running with reasonable time steps, it may be worth adding the strain rate check to future versions of VUMAT A. This has the added benefit of being a material-specific erosion control as opposed to the time-step erosion, which applied globally to all elements in the simulation.

4.2 VUMAT B Cycle Dependence

Alexander et al. (2021) described the gradual failure mechanism used by VUMAT B as a constant decay (parameter A) applied at each cycle. While this was clearly effective at distributing the element failures over time to eliminate the failure cascades, it also implicitly depended on the time step in the simulation. By default, LS-DYNA automatically calculated the time step as 41.7 ns. Additional simulations in which the time step was capped at 10, 20, or 30 ns were run to examine the sensitivity of the results.

Figure 19 shows that there was a significant dependence on the time step. Smaller time steps enabled elements to decay to zero strength more quickly, which manifested as sharper drops in force in the force-displacement curves and faster growth in the total number of failed elements. In practice, this would be unlikely to cause major problems because most simulations use the automatic time-step option, which was in turn primarily driven by the mesh size. Thus, the time step and results when using VUMAT B should be consistent between users and systems unless a more finely meshed object were to be added to the simulation.

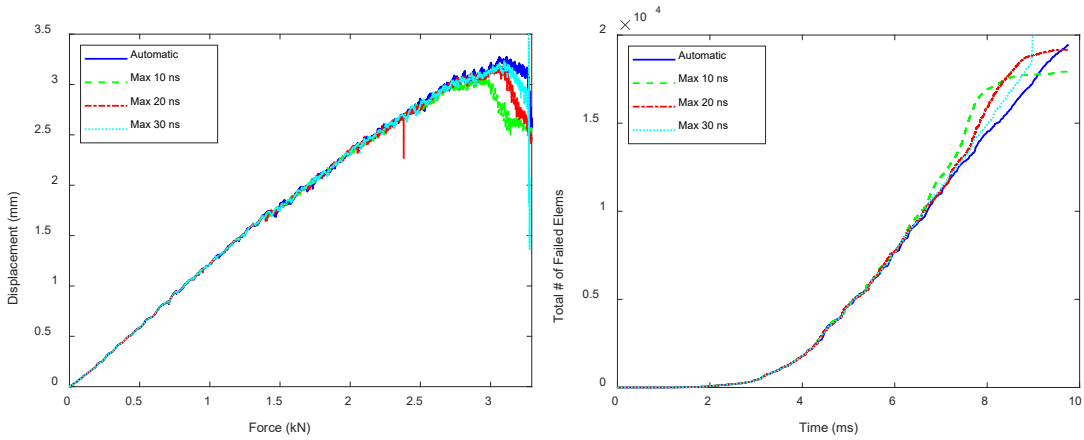

Fig. 19 Force-displacement (left) and total failed elements (right) for skullcap simulations with VUMAT B using different maximum time steps

4.3 Contact Implementation

The bone block simulations used a moving rigid wall to capture the interaction between the block and platen. However, sometimes a more complex loading may be desired that would prevent the use of a rigid wall. In these situations, the most common approach in LS-DYNA would be to mesh the platen and add a sliding contact between the two parts. To test whether this affects the simulation results, the bone block with VUMAT A simulation was repeated with a meshed platen and either a surface-to-surface or node-to-surface sliding contact. The behavior of the bone block was unchanged at the macro level, but some elements were distorted at the element level for the surface-to-surface contact only (Fig. 20). Detection of edges, of which the bone block has plenty, is a known issue for surface-to-surface contacts and is probably the cause of these distorted elements. Simulations with explicitly meshed platens can use the node-to-surface implementation to avoid these problems, and in the bone block simulations there was no difference when using the node-to-surface contact. The skullcap simulations did not have sharp 90° edges as seen in the bone block and did not suffer from any contact issues.

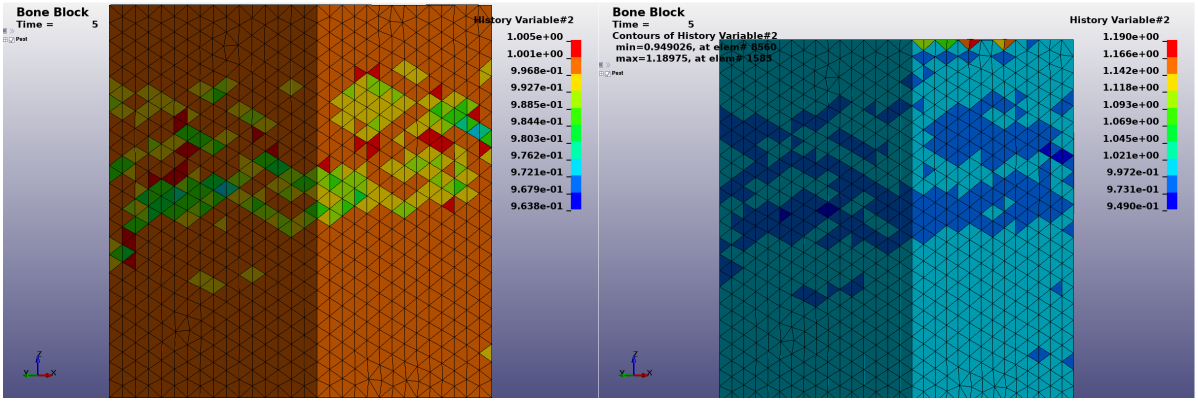

Fig. 20 Relative volume contours for bone block with VUMAT A simulations using a node-to-surface contact (left) or a surface-to-surface contact (right). There were distorted elements along the top edges caused by the surface-to-surface contact.

A quick parametric study was run to examine the effects of certain nonphysical simulation parameters on the simulation results. The first parameters looked at were the bulk viscosity coefficients, which were two numbers describing the linear and quadratic components. The default values of the quadratic term were different between Abaqus (1.2) and LS-DYNA (1.5). However, changing the LS-DYNA parameters to match the Abaqus defaults did not affect the simulations. Similarly, the response to hourglass control in LS-DYNA was checked by changing the default global hourglass formulation (0) to 1, 2, 3, 4, or 5. Again, there was no change when switching the hourglass control. This was expected because the bone block was composed of tetrahedral elements, which are not vulnerable to hourglass modes. They are, however, vulnerable to locking, which was extremely pronounced when the LS-DYNA simulations were run with the default element formulation. This resulted in artificially high forces and effective stiffnesses, so LS-DYNA simulations should always use the tetrahedron-specific element formulation 10. The alternative LS-DYNA tetrahedral formulation, type 13, could not be used because elements with different material models share nodes. This was explicitly discouraged in the keyword manual (LST 2020) and resulted in error terminations when attempted.

4.4 Hardware Effects

Many finite element codes, including the LS-DYNA finite element solver, are optimized to run on specific hardware. For example, this study was run on an executable compiled for Unix on SGI / Intel systems, whereas other executables were compiled for other hardware (e.g., Cray) or operating systems (e.g., Windows). Since the Army computing clusters all use Unix-based operating systems, the effect of Windows executables was not considered. Instead, the user material was ported

from the US Army Centennial system (an SGI / Intel system) to the US Navy Narwhal system (a Cray system) to test hardware effects.

Each of the four test cases run previously were run again on the Narwhal system and compared to the original results from the Centennial system. Figure 21 shows the stress–strain response in the uniaxial compression of bone block simulations as well as the skullcap indentation force-displacement curves. The simulation results were identical in all four cases. Thus, there should not be any issues in porting the material to other clusters using different underlying hardware.

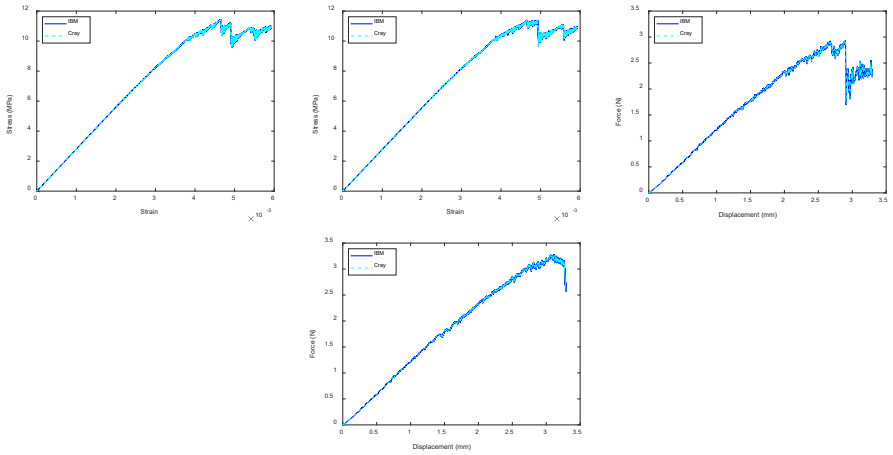

Fig. 21 Repeatability of the four test cases between two different systems

Figure 22 examines how the number of processors used per simulation might affect the results of the most computationally demanding simulation, the skullcap indentation with VUMAT B. Simulations were run using 1, 2, 4, 8, 16, 64, or 128 processors. Higher numbers were not considered since the simulation was not taxing enough to warrant more processors. Figure 22 shows that the force-displacement curves for each simulation were overlaid over top each other, so the number of processors used did not affect the results. The companion plot shows that the real-world time needed to finish each simulation leveled off sharply at 32 processors, after which there was little to gain in adding additional processors.

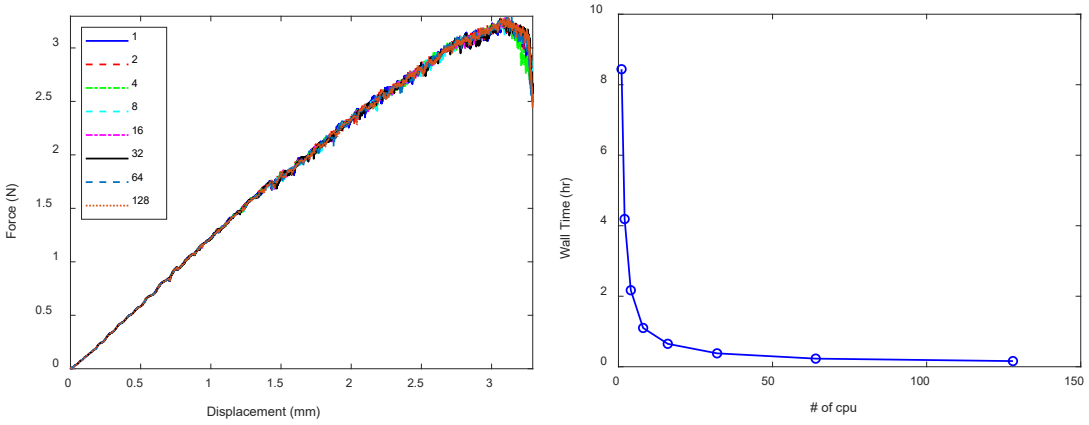

Fig. 22 The repeatability in force-displacement results (left) and the real time needed to complete the simulation (right) when running the skullcap with VUMAT B simulation with different numbers of processors

4.5 Shear Equation Implementation

The different data structures and input were a major challenge in interfacing with finite element software packages. In particular, the limited literature available suggested that Abaqus and LS-DYNA pass the shear components of the incremental strain matrix to the user-defined material routines in a different format. More details on the differences and how the stress equations are formulated are in Appendix E. Omitting the changes in the shear stress equations would be an easily missed error when transferring code between finite element packages.

Two test cases (block with VUMAT A, skullcap with VUMAT B) were rerun with the incorrect shear stress equations to investigate how significantly this would affect the results. Figure 23 shows that the changes were subtle, with the most measurable change being an increase in effective modulus prior to the initiation of element failures. The higher effective stiffness also tended to cause failure cascades (VUMAT A) to occur earlier, but this was not as easily quantified as the change in effective stiffness.

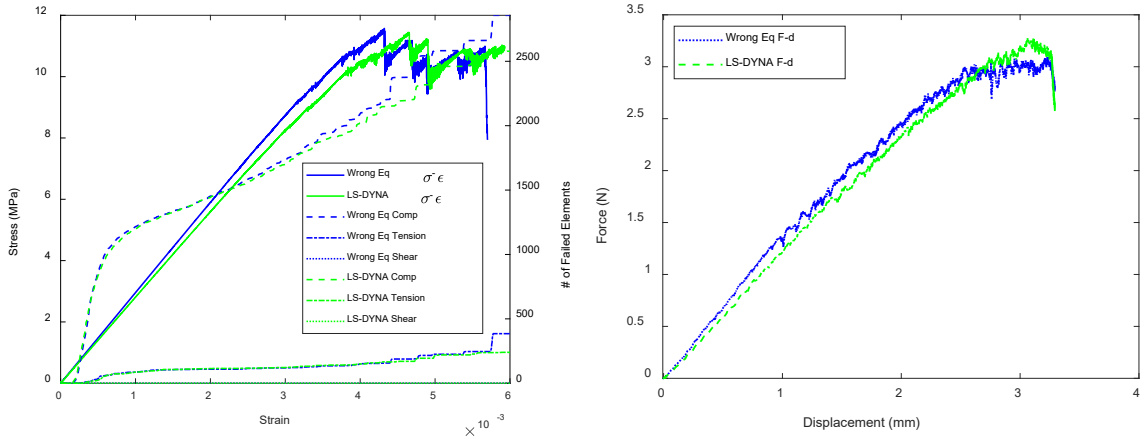

Fig. 23 Effects of changing the shear stress calculations for block with VUMAT A (left) and skullcap with VUMAT B (right)

4.6 Limitations

All of the limitations noted in Alexander et al. (2021) continue to be relevant in this study, as no major changes to the material logic have been implemented. The most pertinent limitation was that the four test cases used to date were near quasistatic in loading. However, a review of the literature for experimentally obtained bone properties (Weerasooriya and Alexander 2021) indicated that rate sensitivity will be needed to expand the material into more dynamic applications. Potential issues with element type (hexahedral vs. tetrahedral) and mesh resolution remain as valid with LS-DYNA as with the original Abaqus material.

5. Conclusions

User-defined material models for human skull bone that were initially created for use in the Abaqus finite element software were successfully converted to equivalent LS-DYNA user-defined material models. The two material models (VUMAT A and VUMAT B) were used to simulate two different specimens (for four total test cases). The results were compared to the previously published results with Abaqus.

The agreement between the two implementations of VUMAT A was excellent, with the visual pattern for failed elements and the force-displacement curve agreeing well between the two finite element solvers. The major caveat while working with VUMAT A was the lack of built-in handling of distorted elements. The easiest resolution was to include time step–based erosion criterion.

The agreement between the two versions of VUMAT B was also good. The visual pattern of failed elements matched well, but there were some differences in the force-displacement history. VUMAT B included an erosion criterion for distorted

elements based on the effective strain rate, which was found to be more effective than the time step–based erosion used with VUMAT A. However, VUMAT B also included a failure-smoothing routine that depended on the number of cycles, which introduced an unexpected dependence on the simulation time step.

An examination of nonphysical simulation parameters revealed that the erosion control for distorted elements was the most influential factor considered and could change both the number of failed elements and the measured force displacement. Simulations with many sharp edges, such as the bone block used in this study, may also be sensitive to the implementation of contact, and a node-to-surface approach avoided distortions observed when using surface-to-surface contacts. Finally, the system used to run the simulations, and the number of processors per simulation, did not have any effect on the results.

The new material models are expected to be available soon for use in unprotected head impact and behind-helmet blunt trauma evaluation, where it is expected that the quasistatic nature of these material models will need to be addressed.

6. References

Alexander SL, Baumer T, Fagan B, Weerasooriya T. Hybrid experimental modeling computational (HEMC) skullcap simulation: elemental to layer simplification and application to microstructural stochasticity. Army Research Laboratory (US); 2021. Report No.: ARL-TR-9296. https://apps.dtic.mil/sti/citations/AD1118637.

Alexander SL, Rafaels K, Gunnarsson CA, Weerasooriya T. Structural analysis of the frontal and parietal bones of the human skull. J Mech Behav Biomed Mater. 2019;90:689–701. https://doi.org/10.1016/j.jmbbm.2018.10.035.

Alexander S, Weerasooriya T. Implementation and validation of finite element model of skull deformation and failure response during uniaxial compression. J Mech Behav Biomed Mater. 2021;115(104302). https://doi.org/10.1016/j.jmbbm.2020.104302.

Gunnarsson CA, Alexander SL, Weerasooriya T. Mechanical response and fracture of human skull to blunt indentation loading. Army Research Laboratory (US); 2021. Report No.: ARL-TR-9142. https://apps.dtic.mil/sti/citations/AD1122025.

Hallquist JO, Whirley RG. DYNA3D user's manual (nonlinear dynamic analysis of structures in three dimensions) UCID--19592-Rev.5. Lawrence Livermore National Laboratory; 1989.

Livermore Software Technology (LST). LS-DYNA keyword user's manual – volume I r:13109 LS-DYNA R12. Livermore Software Technology; 2020.

McElhaney JH. Dynamic response of bone and muscle tissue. J Appl Physiol. 1966;21(4):1231–1236. https://doi.org/10.1152/jappl.1966.21.4.1231.

Weerasooriya T, Alexander S. Mechanism and microstructure based concept to predict skull fracture using a hybrid-experimental-modeling-computational approach. J Mech Behav Biomed Mater. 2021;121(104599). https://doi.org/10.1016/j.jmbbm.2021.104599.

Appendix A. LS-DYNA User Material (VUMAT A)

This is a vectorized LS-DYNA user material implementing isotropic linear elastic equations for porous materials, where the corresponding material properties can be calculated by knowing the volume fraction of the material. This material model can only be used with solid elements.

This material model was originally developed by Alexander and Weerasooriya[1] as an Abaqus user material model called VUMAT A, which describes the material properties of isotropic human cranial bone of varying bone volume fraction (BVF). The material properties of 100% dense cortical bone and two scaling exponents must be provided in order for the scaled material properties to be calculated. This material model is typically used in conjunction with a script that will assign individual elements to one of many materials based on the element's BVF.

This material includes three history variables for the element state, relative volume, and initial BVF, respectively. These variables can be accessed in LS-PrePost or other postprocessing software by setting NEIPH in *DATABASE_EXTENT_BINARY.

All elements initialize to STATE = 1 (healthy element). Individual elements change to a failed state when the principal or shear stresses exceed the scaled stress limits:

- Stress failure limit in compression: SFC = REFSFC * (BVF ^ EXPK)
- Stress failure limit in tension: SFT = REFSFT * (BVF ^ EXPK)
- Stress failure limit in shear: SFS = REFSFS * (BVF ^ EXPK)

An element that has failed is permanently assigned a corresponding STATE of –57 (failed by compression), –75 (failed by tension), or –39 (failed by shear). State values are chosen to ensure sufficient visual differentiation when plotted in a colored contour. These failed states have no relation to LS-DYNA's own internal failure variables that control element erosion.

Once an element has failed, its behavior depends on the relative volume (RELVOL). Failed elements in compression (RELVOL <= 1) can carry bulk loading only. Failed elements in tension (RELVOL > 1) behave differently based on the BVF. If the BVF >= 0.1, then the element carries no load at all, otherwise the element carries bulk loading in an attempt to suppress element distortion.

LS-DYNA requires the initial bulk modulus (INIBLK) and shear modulus (INISHR) for each material in the input cards to support initialization of the element and contact time steps. These values can be calculated with the following equations:

[1] Alexander SL, Weerasooriya T. Implementation and validation of finite element model of skull deformation and failure response during uniaxial compression. J Mech Behav Biomed Mater. 2021;115(104302). https://doi.org/10.1016/j.jmbbm.2020.104302.

$$E = REFMOD * (BVF \wedge EXPN)$$

$$INIBLK = E / (3 * (1 - 2*REFNU))$$

$$INISHR = E / (2 * (1 + REFNU))$$

Card 1 and Card 2: These cards are required for all user-defined materials as described in the *LS-DYNA Keyword User's Manual Vol II*[2] for *MAT_041-050.

Card 1	1	2	3	4	5	6	7	8
Variable	MID	RO	MT	LMC	NHV	IORTHO	IBULK	IG
Type	Integer	Real	Integer	Integer	Integer	Integer	Integer	Integer
Value				14	3	0	7	8

Card 2	1	2	3	4	5	6	7	8
Variable	IVECT	IFAIL	ITHERM	IHYPER	IEOS	LMCA		
Type	Integer	Integer	Integer	Integer	Integer	Integer		
Value	1	0	0	0	0	0		

The following additional cards are required for this user material.

Card 3	1	2	3	4	5	6	7	8
Variable	BVF	EXPN	EXPK				INIBLK	INISHR
Type	Real	Real	Real				Real	Real

Card 4	1	2	3	4	5	6	7	8
Variable	REFRO	REFMOD	REFNU	REFSFC	REFSFT	REFSFS		
Type	Real	Real	Real	Real	Real	Real		

Variable	Description
BVF	The bone volume fraction
EXPN	The scaling exponent in the calculation of the elastic modulus
EXPK	The scaling exponent in the calculation of the current stress failure limits
INIBLK	The initial bulk modulus, used only for calculating initial time step
INISHR	The initial shear modulus, used only for calculating initial time step
REFRO	The density of 100% dense bone
REFMOD	The Young's (elastic) modulus of 100% dense bone
REFNU	The Poisson's ratio of 100% dense bone
REFSFC	The stress failure limit in compression for 100% dense bone Set to a large value to disable this failure mode
REFSFT	The stress failure limit in tension for 100% dense bone Set to a large value to disable this failure mode
REFSFS	The stress failure limit in shear for 100% dense bone Set to a large value to disable this failure mode

[2] Livermore Software Technology (LST). LS-DYNA keyword user's manual – volume II. Livermore Software Technology; 2017.

Appendix B. LS-DYNA User Material (VUMAT B)

This is a vectorized LS-DYNA user material implementing isotropic linear elastic equations for porous materials, where the corresponding material properties can be calculated by knowing the volume fraction of the material. This material model can only be used with solid elements.

This material model was originally developed by Alexander et al.[1] as an Abaqus user material model called VUMAT B, which describes the material properties of isotropic human cranial bone of varying bone volume fraction (BVF). It differs from the previously developed VUMAT A[2] by including time-dispersed damage scaling of the material properties for elements failing in tension. The material properties of 100% dense cortical bone and two scaling exponents must be provided in order for the scaled material properties to be calculated. This material model is typically used in conjunction with a script that will assign individual elements to one of many materials based on the element's BVF.

This material includes three history variables for the element state, relative volume, and health, respectively. These variables can be accessed in LS-PrePost or other postprocessing software by setting NEIPH in *DATABASE_EXTENT_BINARY.

All elements initialize to STATE = 1 and HEALTH = 1 (healthy element). Individual elements change to a failed state when the principal stresses exceed the following scaled stress limits:

- Stress failure limit in compression: SFC = REFSFC * (BVF ^ EXPK)
- Stress failure limit in shear: SFS = REFSFS * (BVF ^ EXPK)
- First stress failure limit in tension: SFT = REFSFT * (BVF ^ EXPK)
- Second stress failure limit in tension: SFR = REFSFR * (BVF ^ EXPK)

An element that has failed is assigned a corresponding state of 0 (100% failed by tension), –57 (failed by compression), –75 (partially failed by tension), or –39 (failed by shear). These failed states have no relation to LS-DYNA's own internal failure variables that control element erosion.

In VUMAT B, elements that exceed SFT but not SFR are assigned a new health based on the max principal stress (SMAX) as shown in the equation below. The

[1] Alexander SL, Baumer T, Fagan B, Weerasooriya T. Hybrid experimental modeling computational (HEMC) skullcap simulation: elemental to layer simplification and application to microstructural stochasticity. Army Research Laboratory (US); 2021. Report No.: ARL-TR-9296.

[2] Alexander SL, Weerasooriya T. Implementation and validation of finite element model of skull deformation and failure response during uniaxial compression. J Mech Behav Biomed Mater. 2021;115(104302).

health of the element will then degrade by a fixed scale factor (A) for each subsequent time step under tension. During this process, the element will behave as a healthy element with the modulus scaled by HEALTH. Once HEALTH falls below a minimum threshold (HFLR), the element is fully failed and the HEALTH and STATE are set to zero.

$$HEALTH = (SFR-SMAX) / (SFR-SFT)$$

Once an element has failed, its behavior depends on the relative volume (RELVOL). Failed elements in compression (RELVOL <= 1) can carry bulk loading only. Fully failed elements in tension (RELVOL > 1) behave differently based on the BVF. If the BVF >= 0.1, then the element carries no load at all, otherwise the element carries bulk loading in an attempt to suppress element distortion.

LS-DYNA requires the initial bulk modulus (INIBLK) and shear modulus (INISHR) for each material in the input cards to support initialization of the element and contact time steps. These values can be calculated with the following equations:

$$E = REFMOD * (BVF \wedge EXPN)$$

$$INIBLK = E / (3 * (1 - 2*REFNU))$$

$$INISHR = E / (2 * (1 + REFNU))$$

Card 1 and Card 2: These cards are required for all user-defined materials as described in *LS-DYNA Keyword User's Manual Vol II*[3] for *MAT_041-050.

Card 1	1	2	3	4	5	6	7	8
Variable	MID	RO	MT	LMC	NHV	IORTHO	IBULK	IG
Type	Integer	Real	Integer	Integer	Integer	Integer	Integer	Integer
Value				15	3	0	7	8

Card 2	1	2	3	4	5	6	7	8
Variable	IVECT	IFAIL	ITHERM	IHYPER	IEOS	LMCA		
Type	Integer	Integer	Integer	Integer	Integer	Integer		
Value	1	0	0	0	0	0		

The following additional cards are required for this user material.

Card 3	1	2	3	4	5	6	7	8
Variable	BVF	EXPN	EXPK	SRATE	A	HFLR	INIBLK	INISHR
Type	Real	Real	Real	Real	Real	Real	Real	Real

[3] Livermore Software Technology (LST). LS-DYNA keyword user's manual – volume II. Livermore Software Technology; 2017.

Card 4	1	2	3	4	5	6	7	8
Variable	REFRO	REFMOD	REFNU	REFSFC	REFSFT	REFSFS	REFSFR	
Type	Real	Real	Real	Real	Real	Real	Real	

Variable	Description
BVF	The bone volume fraction
EXPN	The scaling exponent in the calculation of the elastic modulus
EXPK	The scaling exponent in the calculation of the current stress failure limits
SRATE	Elements that exceed this effective strain rate will be eroded; typically used to catch highly distorted, low BVF elements
A	Elements that have previously failed by tension and are currently in tension will have their health scaled each cycle by A
HFLR	Elements that have previously failed by tension and are currently in tension will be considered fully failed when the element health falls below HFLR
INIBLK	The initial bulk modulus, used only for calculating initial time step
INISHR	The initial shear modulus, used only for calculating initial time step
REFRO	The density of 100% dense bone
REFMOD	The Young's (elastic) modulus of 100% dense bone
REFNU	The Poisson's ratio of 100% dense bone
REFSFC	The stress failure limit in compression for 100% dense bone
REFSFT	The first stress failure limit in tension for 100% dense bone, after which element damage will begin to accumulate
REFSFS	The stress failure limit in shear for 100% dense bone
REFSFR	The second stress failure limit in tension for 100% dense bone, at which an element would instantly sustain 100% damage and transition to a failed state

Appendix C. Compiling and Running on a Computing Cluster

This study's user material model was implemented for use on high-performance-computing clusters. Such systems are typically parallelized to break down large, complex problems into more manageable chunks that can be computed faster. In this study, the user material was written with MPI (Message Passing Interface) in mind.

It is assumed that the target system will have software modules available for access to various programming tools and stock versions of LS-DYNA finite element solver. It is recommended to read Appendix A of the *LS-DYNA User's Keyword Manual*[1] for further details on implementing LS-DYNA user materials.

C.1 Making Modifications to the Code

The vast majority of the LS-DYNA source code is written in the older Fortran 77 (fixed width) format. There are a number of oddities in writing code that users should be aware of:

- The first six characters are reserved for comment markers (c) or numbers indicating continuation of a statement over multiple lines.
- The width of any line cannot exceed 80 characters.
- Variable type declarations must occur before assigning initial values or performing operations.
- Un-typed variables beginning with the letters i, j, k, l, m, or n will become integers, and all others will become real numbers. This behavior can be avoided by explicitly declaring the type.
- Some of the example materials in the unmodified umat files are incomplete and meant to be filled in by attending the training classes offered on implementing user materials.

To deploy the vectorized user material models described in this study, the source code should be inserted into the dyn21umatv.f file, replacing the contents of one of the existing materials. In this study, we have chosen to replace umat41v with VUMAT A and umat44v with VUMAT B.

[1] Livermore Software Technology (LST). LS-DYNA keyword user's manual – volume I r:13109 LS-DYNA R12. Livermore Software Technology; 2020.

C.2 Compiling

Any previously compiled object files (*.o) must be deleted prior to compiling via running the "make" file. Additionally, to compile the modified LS-DYNA executable, the following modules are needed:

- A Fortran compiler (compiler/intel/16.0.4.258 in this study)
- An MPI package (mpi/intelmpi/2018.0.128 for this study)

Compiling can then be initiated with the command "make." No additional arguments are needed.

C.3 Execution

Running an LS-DYNA simulation with the new user material is very similar to running a simulation with the predefined LS-DYNA modules, with the following caveats: (1) the two modules described previously must also be loaded when attempting to run the newly compiled executables, (2) load one of the predefined LS-DYNA modules to access the licenses, and (3) your $PATH variable must include the directory containing the new LS-DYNA executable.

Appendix D. List of Simulations

Series	Simulation name	Specimen	VUMAT	Completion (%)	Wall time (min)
Baseline	BlockA	Bone block	A	100	5.38
	BlockB	Bone block	B	100	5.27
	SkullcapA	Skullcap	A	100	50.62
	SkullcapB	Skullcap	B	100	22.72
Repeat	RepeatBA	Bone block	A	100	5.43
	RepeatBB	Bone block	B	100	5.37
	RepeatSA	Skullcap	A	100	50.22
	RepeatSB	Skullcap	B	100	22.98
Hard-ware	NarwhalBA	Bone block	A	100	3.52
	NarwhalBB	Bone block	B	100	2.97
	NarwhalSA	Skullcap	A	100	25.32
	NarwhalSB	Skullcap	B	100	11.28
Abaqus ShearCalc	FullBA	Bone block	A	96	60
	FullBB	Bone block	B	100	4.37
	FullSA	Skullcap	A	100	33.33
	FullSB	Skullcap	B	100	22.68
CPU Scaling	Cpu001	Skullcap	B	100	506.31
	Cpu002	Skullcap	B	100	251.58
	Cpu004	Skullcap	B	100	130.16
	Cpu008	Skullcap	B	100	66.00
	Cpu016	Skullcap	B	100	38.90
	Cpu064	Skullcap	B	100	13.80
	Cpu128	Skullcap	B	100	9.60
Erosion	ErosionNone	Skullcap	B	65	240.00
	ErosionDt	Skullcap	B	100	23.73
	ErosionDtSr	Skullcap	B	100	23.52
Time step	Time step 10 ns	Skullcap	B	100	85.70
	Time step 20 ns	Skullcap	B	100	48.58
	Time step 30 ns	Skullcap	B	95	120.00

Appendix E. Equivalence of LS-DYNA and Abaqus Stress Equations

In this section, ε will refer to the incremental strain as calculated by the finite element codes rather than the engineering strain.

The derivation of the finite element–ready equations of linear elasticity from the general theory of elasticity was outside the scope of this study, but a condensed overview can be reviewed if needed.[1]

E.1 Bulk Stress

The Abaqus user material implementation of linear elasticity calculates the axial stress components as follows:

$$\sigma_{k,t} = \sigma_{k.t-1} + \frac{E}{1+v}\varepsilon_k + \frac{Ev}{(1-2v)(1+v)}(\varepsilon_1 + \varepsilon_2 + \varepsilon_3) \quad \text{for k=1,2,3} \qquad \text{(E-1)}$$

This approach places emphasis on the Lamé parameters μ and λ, where

$$\mu = \frac{E}{2(1+v)} \qquad \text{and} \qquad \lambda = \frac{Ev}{(1-2v)(1+v)} \qquad \text{(E-2)}$$

In contrast, the LS-DYNA implementation is as follows:

$$\sigma_{k,t} = \sigma_{k,t-1} + \frac{E(\varepsilon_1+\varepsilon_2+\varepsilon_3)}{3(1-2v)} + \frac{E}{(1+v)}\left(\varepsilon_k - \frac{\varepsilon_1+\varepsilon_2+\varepsilon_3}{3}\right) \quad \text{for k=1,2,3} \qquad \text{(E-3)}$$

This approach highlights the volumetric and deviatoric components of the stress, and the commonly used shear (G) and bulk (K) moduli, where

$$G = \mu = \frac{E}{2(1+v)} \qquad \text{and} \qquad K = \frac{E}{3(1-2v)} \qquad \text{(E-4)}$$

At first glance, Eq. E-3 is not obviously equivalent to the Abaqus method (Eq. E-1) for calculating axial stress components. However, looking at Eq. E-3 for k = 1, the final term can be distributed to remove the parentheses:

$$\sigma_{1,t} = \sigma_{1,t-1} + \frac{E}{1-2v}\frac{\varepsilon_1+\varepsilon_2+\varepsilon_3}{3} + \frac{E}{1+v}\varepsilon_1 + \frac{E}{1+v}\frac{-\varepsilon_1-\varepsilon_2-\varepsilon_3}{3} \qquad \text{(E-5)}$$

In order to combine the second and fourth terms, the second term was multiplied by (1+v)/(1+v) and the fourth term by (1-2v)/(1-2v). This yields

$$\sigma_{1,t} = \sigma_{1,t-1} + \frac{E(1+v)}{(1-2v)(1+v)}\frac{\varepsilon_1+\varepsilon_2+\varepsilon_3}{3} + \frac{E}{1+v}\varepsilon_1 - \frac{E(1-2v)}{(1+v)(1-2v)}\left(\frac{\varepsilon_1+\varepsilon_2+\varepsilon_3}{3}\right) \qquad \text{(E-6)}$$

Parameters common to both the second and fourth terms can be pulled out, and the equation rearranged to give

$$\sigma_{1,t} = \sigma_{1,t-1} + \frac{E}{1+v}\varepsilon_1 + \frac{\varepsilon_1+\varepsilon_2+\varepsilon_3}{3(1+v)(1-2v)}[E(1+v) - E(1-2v)] \qquad \text{(E-7)}$$

[1] Brown University. Mechanics of elastic solids; 2022 [accessed 28 Mar 2022]. https://www.brown.edu/Departments/Engineering/Courses/En221/Notes/Elasticity/Elasticity.htm.

Expanding the terms inside the bracket will eliminate some terms, and the others

$$E + Ev - E + 2Ev = 3Ev$$

Reducing the full equation to

$$\sigma_{1,t} = \sigma_{1,t-1} + \frac{E}{1+v}\varepsilon_1 + \frac{Ev}{(1+v)(1-2v)}(\varepsilon_1 + \varepsilon_2 + \varepsilon_3)$$

which is the same as the Abaqus implementation shown in Eq. E-1 for k = 1, 2, and 3.

E.2 Shear Stress

Further ambiguity was encountered in the calculation of the shear stress components. The Abaqus implements these calculations as

$$\sigma_{k,t} = \sigma_{k,t-1} + 2G\epsilon_k \qquad \text{for k = 4,5,6} \qquad \text{(E-8)}$$

However, the LS-DYNA default implementation is

$$\sigma_{k,t} = \sigma_{k,t-1} + G\epsilon_k \qquad \text{for k = 4,5,6} \qquad \text{(E-9)}$$

In both cases G is the shear modulus described previously in Eq. E-4. The difference in implementation arises from the way in which the incremental shear strains are passed to the user material. The Abaqus Version 6.6 documentation on 1.2.4 VUMAT states that Abaqus passes in the tensorial shear increments as the following:

$$\epsilon_4 = \frac{\partial u}{\partial y} \qquad \epsilon_5 = \frac{\partial v}{\partial z} \qquad \epsilon_6 = \frac{\partial w}{\partial x}$$

No documentation could be found on how the shear strain increments were passed in the LS-DYNA User Manuals (Volume I-III). However, a user frequently-asked-questions document[2] (LST 2021) contained this exact query, where it was stated that LS-DYNA passes them in as

$$\epsilon_4 = \frac{\partial u}{\partial y} + \frac{\partial v}{\partial x} \qquad \epsilon_5 = \frac{\partial v}{\partial z} + \frac{\partial w}{\partial y} \qquad \epsilon_6 = \frac{\partial u}{\partial z} + \frac{\partial w}{\partial x}$$

Since the finite element codes operate under the assumption that the strain and stress tensors are symmetric, these LS-DYNA strain terms were double those of the Abaqus strain terms. Thus, the LS-DYNA user material implementation must calculate the updated shear stress components using G rather than 2G to match the Abaqus user material calculations.

[2] LST. user_defined_materials.faq; 2018 Apr 4 [accessed 2021 Nov 08]. https://ftp.lstc.com/anonymous/outgoing/support/FAQ/user_defined_materials.faq.

List of Symbols, Abbreviations, and Acronyms

σ	engineering stress
ε	engineering strain
ρ	density
ν	Poisson's ratio
ARL	Army Research Laboratory
BVF	bone volume fraction
DEVCOM	US Army Combat Capabilities Development Command
E	elastic modulus/ Young's modulus
G	shear modulus
K	bulk modulus
MPI	Message Passing Interface

1 (PDF) DEFENSE TECHNICAL INFORMATION CTR DTIC OCA

1 (PDF) DEVCOM ARL FCDD RLD DCI TECH LIB

30 (PDF) DEVCOM ARL FCDD RLR EM A BROWN FCDD RLW J ZABINSKI FCDD RLW B C HOPPEL P GILLICH FCDD RLH BA A EIDSMORE FCDD RLW MA T PLAISTED E WETZEL FCDD RLW T R FRANCART FCDD RLW TB S ALEXANDER R BANTON T BAUMER B FAGAN A GOERTZ A GUNNARSSON C HAMPTON R KARGUS D KRAYTERMAN M KLEINBERGER E MATHEIS JR MCDONALD P MCKEE K RAFAELS S SATAPATHY M TEGTMEYER C WEAVER T WEERASOORIYA S WOZNIAK T ZHANG FCDD RLW TG N GNIAZDOWSKI S KUKUCK